9. SUPERCONDUCTING RF LINACS

Choice of RF Technology

The baseline recirculating linac design requires acceleration through four passes in a 600 MeV linac up to a final energy of 2.5 GeV. A 1 nC bunch is launched from the rf photocathode gun at a 10 kHz rate, and passes through the linac four times to give an average current of 40 μA in the main linac.

Tremendous progress has been made in both superconducting and normal conducting rf linac technology in recent years, mainly resulting from research on linear collider projects. The proposed linac design should take advantage of these developments.

Research on superconducting structures for the TeV-Energy Superconducting Linear Accelerator (TESLA) project has greatly advanced the technology [1]. Accelerating gradients of 42 MV/m have been achieved in an electro-polished seamless single cell Nb cavity at 1.3 GHz, and 9-cell TESLA cavities have been tested at gradients exceeding 25 MV/m and with unloaded quality factors Q_0 over 10^{10}. More recently an electro-polished 9-cell Nb cavity has reached a record gradient of 32 MV/m [2].

The development of copper structures has a long history and the technology is relatively mature. In recent years the Next Linear Collider (NLC) project has led the field in research on room temperature copper rf structures for high-gradient linacs, and gradients of over 50 MV/m have been demonstrated at 11.4 GHz although rf breakdown was observed around 70 MV/m in some structures [3]. The SLAC S-band (2.856 GHz) linac has been running successfully at ~20 MV/m for decades.

In principle, both superconducting and normal warm copper structures are capable of providing the required accelerating gradient for the re-circulating linac although they each raise different technical challenges. Table 9-1 summarizes parameters for several linac options assuming using either superconducting (SC) or normal conducting (NC) rf technologies.

For the NC rf approach, SLAC S-band and X-band traveling wave (TW) linac parameters are used, assuming a 3□ filling time without flat top for all the calculations. The NC L-band linac calculations were scaled from the SLAC S-band linac parameters. For the SC linac, parameters for the TESLA Test Facility (TTF) cryomodule are used.

The large quality factors for the SC structures ($Q_0 \sim 10^{10}$) result in a very long filling time (>1 ms at 1.3 GHz), and the SC linac must be operated in continuous wave (CW) mode for the required 10 kHz bunch repetition rate (100 μs time interval). The resultant power dissipation due to rf currents on the cavity inner surfaces increases significantly over the TESLA design parameters, and implications will be discussed in Chapter 13-Cryogenics. A cryogenic system of approximately 3.5 MW capacity is required for operations of the whole facility at 20 MV/m.

Conventional room temperature linacs can be operated in pulsed mode at 10 kHz, but require ~10^3 increase in peak rf power over the SC linac. Operating at high duty factor of approximately 8%, and dissipating ~1 MW/m average rf power, such linacs are technically very demanding and are not known to exist for such applications.

To preserve beam emittance, the influence of wakefields in the linac must be minimized. Wakefield amplitude scales with frequency as $W_L \mu f^2$ and $W_T \mu f^3$, where W_L and W_T denote longitudinal and transverse wakefield, respectively. The lower frequency linac thus has a significant advantage in terms of beam dynamics.

Even at the same resonant frequency, normal conducting cavities usually have optimized geometry to provide much larger R/Q values compared to super-conducting cavities, in order to improve the efficiency of the structure (maximized accelerating voltage per unit input power, and minimized wall losses). The large R/Q leads to increased wakefield amplitude and higher loss factors. For superconducting cavities, however, the cavity geometry is optimized to eliminate multipacting and field emission, since quality factor Q may be many orders of magnitude higher than for copper cavities cavities, and R/Q is not as significant a concern.

Table 9-1 Comparisons between superconducting (SC) and normal conducting (NC) rf systems for a 600 MeV linac

Parameter	NC S-Band	NC L-Band	NC X-Band	SC L-Band
Frequency [GHz]	2.856	1.3	11.4	1.3
Phase Advance	2π/3 (TW)	2π/3 (TW)	2π/3 (TW)	π (SW)
Shunt Impedance [MΩ/m]	50	34	80	~ 10^7
Accelerating Gradient [MV/m]	20	20	50	20
Pulse Length [μs]	2.5	8.1	0.3	CW
Quality Factor (unloaded)	15,000	22,000	7,000	10^{10}
Quality Factor (loaded)	7,500	11,000	3,500	2.6×10^7
Linac Length (active) [m]	30	30	12	33
Filling time $\tau = (2Q_L/\omega)$ [μs]	8.3	2.7	0.098	~ 3180
Repetition Rate [Hz]	10,000	10,000	10,000	CW
Duty Factor	2.5%	8.1%	0.3%	CW
Total Peak RF Power [MW]	240	354	375	0.288
Total Average RF Power [MW]	6	29	1.13	0.288

Based on these considerations superconducting rf linac technology has been chosen for the recirculating linac, and our design is based on TESLA 1.3 GHz cavities and cryomodules [1].

Linac Design

The linac design is based on superconducting rf technology developed for the TESLA project [1]. We propose to use modules similar to those designed for the TESLA-FEL injector to take advantage of the developments made by the TESLA collaboration in obtaining high gradient accelerator cavities, and to avoid an expensive and time-consuming R&D program. The TESLA cavity parameters are well suited to our requirements, and many complex issues including higher-order mode damping, suppression of multipacting, cavity materials preparation and fabrication, input power coupler design, have been studied and solutions explored.

We also follow developments in the Continuous Electron Beam Accelerator Facility (CEBAF) upgrade project at Jefferson Laboratory. The CEBAF upgrade module incorporates 7-cell cavities at 1.5 GHz and aims at 20 MV/m. This design could prove to be a viable choice in the future.

Figure 9-1 shows the cross-section schematic view of a TESLA 9-cell superconducting rf (scrf) cavity [1]. Eight such cavities are integrated with cryogenics and other systems into a TESLA FEL injector linac cryomodule, with cross-section (end view) shown in Figure 9-2. Each of these cryomodules is approximately 12 m long, and four such cryomodules are required to achieve a total energy of $\geq$ 2400 GeV, i.e. $\geq$ 600MeV per pass. We will operate slightly off-crest of the rf field maximum and the design considerations here are for a peak accelerating gradient of 20 MV/m. Operating at the TESLA gradient of 23 MV/m would allow a final beam energy of ~3 GeV, but the lower energy gain provides a design margin and reduces the power dissipation in the cryostat.

The injector linac consists of an additional cryomodule, with reduced gradient of 15 MV/m providing a total energy gain of 110 MeV.

The superconducting cavities have a high intrinsic quality factor ($Q_0 \sim 10^{10}$) resulting in a cavity time constant of about 2.4 seconds. The effective time constant of an SC cavity in the circuit environment is two to three orders of magnitude lower since determined by the *loaded Q*, the choice of which is discussed below. Typically, power is applied to standing wave cavities about three time constants before the beam enters the structure. This allows time for energy to build up in the cavity so that the required field can be developed. Since we want to operate at bunch rates of 10 kHz and greater, the resulting repetition time of 100 μs is much too short to change the field in the cavities commensurately.

The linac rf system must therefore be operated in continuous wave (CW) mode. This, of course, increases the average power requirements of the system, both in terms of the rf drive power and the cryogenic system power, which is needed to absorb the wall losses in the cavities.

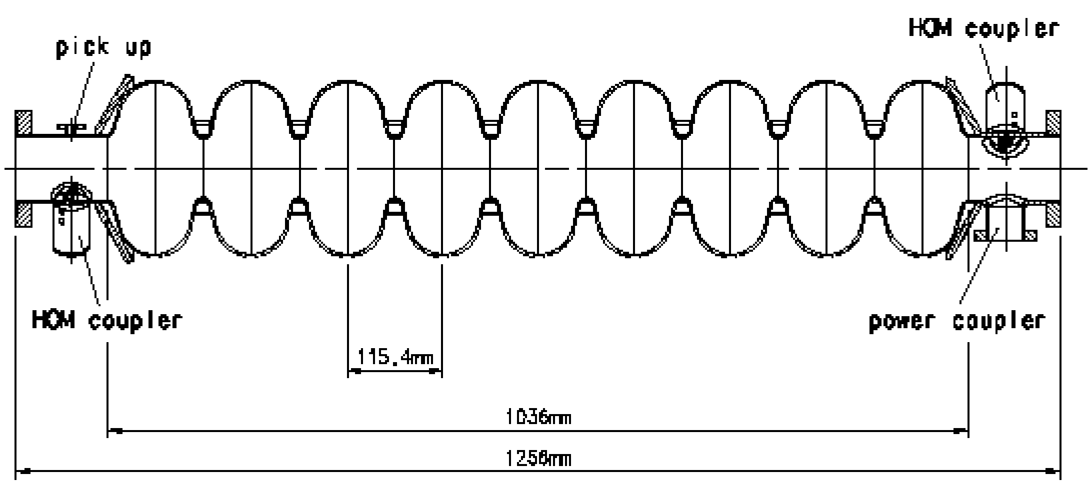

Figure 9-1 TESLA 9-cell superconducting 1.3 GHz cavity, longitudinal cross-section.

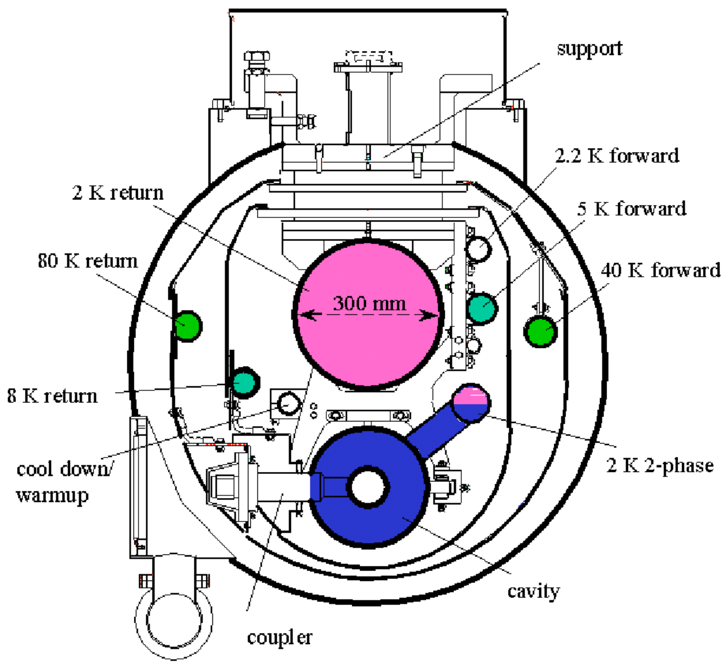

Figure 9-2   TESLA cryomodule end view cross-section

There are a total of 32 cavities in the baseline design 600 MeV main linac, therefore the accelerating voltage for on-crest acceleration is 600/32 = 18.75 MV per cavity. Operation off-crest by as much as 10° brings this to ~19 MV. Together with a nominal length of 1.038 m per cavity the nominal gradient is 18.34 MV/m. To provide some safety margin these figures are rounded respectively to 20 MV per cavity and 20 MV/m cavity gradient.

Tuning Variations of the TESLA Cavity

The basic parameters of the TESLA cavity are

f_{rf} = 1300 MHz,

$Q_0 = 1 * 10^{10}$,

$R/Q = 518\ \Omega$ (equivalent circuit definition $R/Q = V^2/(2\omega U)$)

The intrinsic 3-dB bandwidth of the TESLA cavity is then

$$BW_0 = \frac{f_{rf}}{Q_0} \approx \frac{1300 \cdot 10^6}{10^{10}} \approx 0.13\ Hz \tag{1}$$

The big problem for the use of superconducting cavities is the fact that systematic as well as random tuning errors are orders of magnitude larger than this intrinsic bandwidth.

An example for the systematic part is by the detuning by the radiation pressure forces or *Lorentz force detuning*, given by [4]

$$\frac{\partial f}{\partial U^2} \approx 0.9 \frac{Hz}{\left(\frac{MV}{m}\right)^2} \tag{2}$$

This effect is as large as 360 Hz for a gradient of 20 MV/m. It is of great concern for pulsed cavities, but can be easily corrected in the present application where the field is continuous.

More serious are the random tuning deviations. Figures 9-3 through 9-5 below show measurements taken at a TTF cryomodule [4].

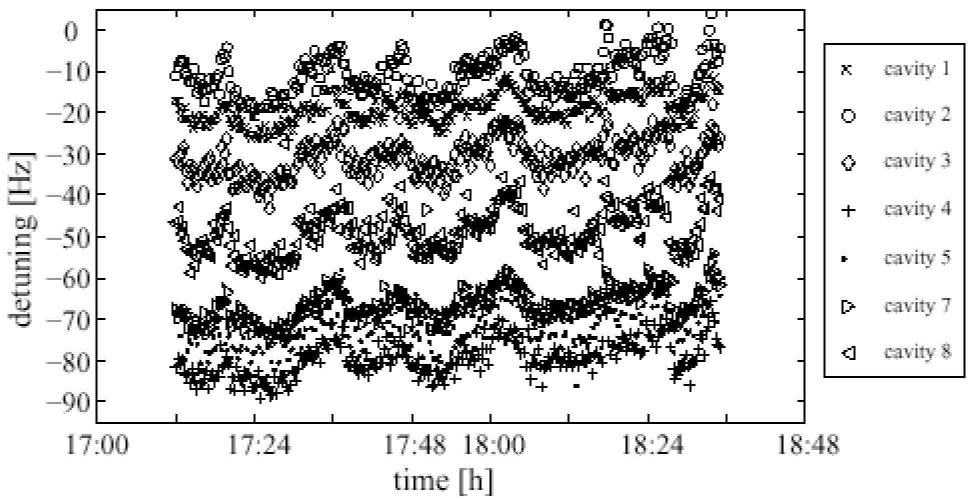

Figure 9-3 Longterm variation of the resonant frequency of the eight cavities in a TTF cryomodule.

The random tuning perturbations fall in two categories:

A. <u>Relatively slow perturbations</u>, with periodic intervals in the minute range. The detuning of all eight cavities is highly correlated; this hints at random variations of the helium pressure as the common cause. The cavity resonant frequency and the pressure variations are related by the factor

$$\frac{\partial f}{\partial p} \approx 20 \frac{Hz}{mbar} \tag{3}$$

The behavior of cavity #1 is shown in detail in Figure 9-4.

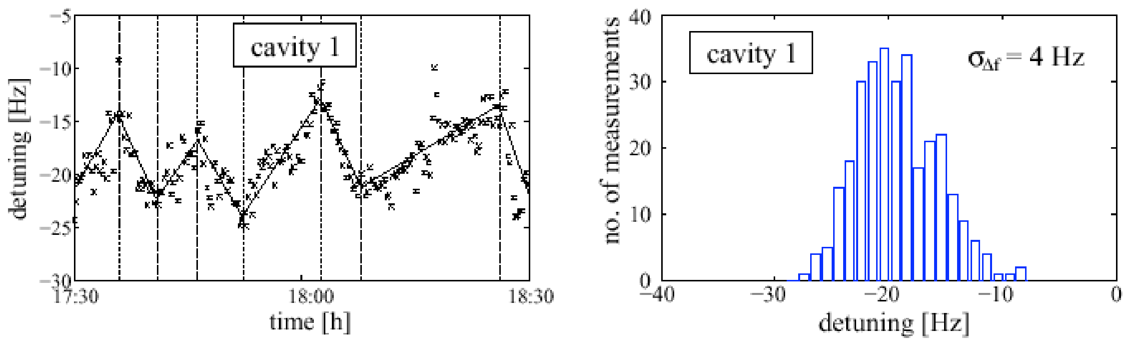

Figure 9-4 Resonant frequency variation of cavity #1 (left), and corresponding histogram (right)

The periodic tuning variations are shown on the left, together with the assumed contribution of the helium pressure changes which are represented by straight lines. A histogram of the uncorrected raw data points is given on the right, showing a standard deviation of $\sigma_{\Delta f} = 4$Hz and a mean tuning error of 19 Hz

B. <u>Fast perturbations</u> due to microphonics in the acoustical frequency range, caused by mechanical stimuli (pumps, turbulence in the helium flow etc). The response is shaped by structural resonances and directional sensitivities of the cavities. Figure 9-5 shows synthesized histograms that consider only these small "residual microphonics" around the triangular lines in Figure 4 (left). It is assumed that the slow variations have been eliminated by a mechanical tuner, with control bandwidth ~1Hz.

The fact that these histograms show a Gaussian-like distribution is a strong hint that they are created by a multitude of uncorrelated resonances, since single resonances would lead to peaks at the tails of the distribution [4]. The results are summarized in Table 9-2.

Table 9-2 Microphonic levels of the cavities in the TTF cryomodule; total rms error, and rms error after elimination of low frequency components

Cavity no.	$\sigma_{\Delta f}$ (rms) raw data	$\sigma_{\Delta f}$ (rms) slow error eliminated	Cavity no.	$\sigma_{\Delta f}$ (rms) raw data	$\sigma_{\Delta f}$ (rms) slow error eliminated
1	4 Hz	2 Hz	5	9 Hz	7 Hz
2	5.5 Hz	4 Hz	6	(detuned)	(detuned)
3	5 Hz	3 Hz	7	4.5 Hz	3 Hz
4	7 Hz	6 Hz	8	6.5 Hz	5 Hz

As a basis for the design of the rf system, we take as a reference the performance of cavity #5 which shows the largest residual microphonics of $\sigma_{\Delta f}$ = 7 Hz (corrected for slow variations). The largest fast tuning variation is expected $3 \cdot \sigma_{\Delta f} \sim 20$ Hz. It appears realistic to assume that the slow tuning offsets can be reduced to ~5 Hz, and it is further assumed that these two components add linearly. The total tuning excursion to be taken into account is therefore about 25 Hz.

It may be tacitly assumed that through additional R&D future generations of superconducting cavities will show equal or superior microphonics characteristics than the units considered here.

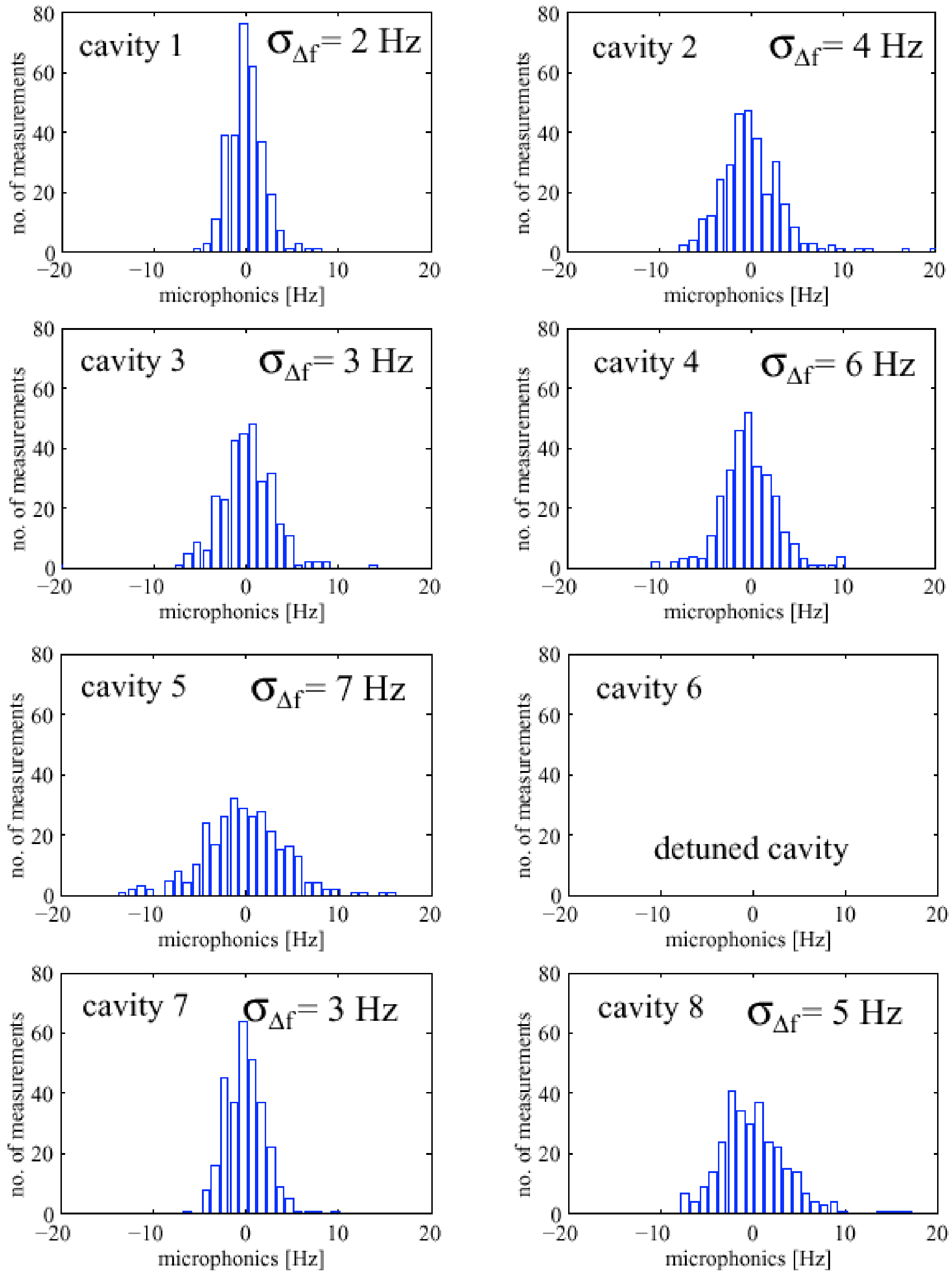

Figure 9-5 Microphonics in the TTF module (helium pressure variations compensated by hypothetical tuner)

Choice of the Cavity Coupling Factor

The coupling between the SC cavity and the rf generator determines the overall system bandwidth and is therefore a key factor for the ability of the rf system to cope with cavity tuning variations. The amount of coupling is usually expressed in terms of the coupling factor β, defined as

$$\beta = \frac{r_{shunt} / k^2}{Z} \tag{5}$$

where Z is the characteristic impedance of the input power feed line, r_{shunt}/k^2 is the cavity shunt impedance (circuit convention) transformed to the input line by the voltage transmission factor k of the coupler.

In other words, β is the mismatch factor or voltage standing wave ratio (VSWR) of the cavity input port with respect to the generator impedance Z, and $\beta=1$ would lead to a perfect match of the bare cavity exempt of beam loading.

Klystrons have to be protected against load mismatch by a circulator or isolator, which in turn provides an almost ideal generator output impedance Z (usually 50 Ω). The overall impedance at any plane of the system is given the parallel connection of transformed generator impedance Z and transformed cavity impedance. It can be easily shown that the real part of impedance at resonance is reduced by the factor (1+ β).

It follows then

$$Q_L = \frac{Q_0}{1+\beta} \tag{6}$$

where Q_L is the *loaded Q* of the cavity/generator assembly. The *loaded* 3-dB bandwidth BW_L of the overall combination becomes

$$BW_L = \frac{f_r}{Q_L} = BW_0 * (1+\beta) \tag{7}$$

The rf system must provide sufficient generator power to establish the nominal field in the cavity under worst-case conditions, i.e. for full detuning by microphonics. The rf power requirement P_g can be expressed analytically by [5]

$$P_g = \frac{P_c}{4\beta} \left\{ (1+\beta+b)^2 + \left[2\, Q \frac{\Delta f}{f} - b \tan(\phi_B) \right]^2 \right\} \tag{8}$$

where P_C is the cavity wall dissipation (42 W), b is the ratio beam power/cavity wall power, ϕ_B is the beam stable phase from crest (0).

For the purpose of investigating capabilities of the system, and adequately specifying components for possible future upgrades, we consider three operating scenarios with varying beam current. Figure 6 shows the necessary generator power for the scenarios of 1 nC at 10 kHz, 3 nC at 10 kHz, and 3 nC at 100 kHz, as a function of the coupling factor, with the detuning Δf as a parameter.

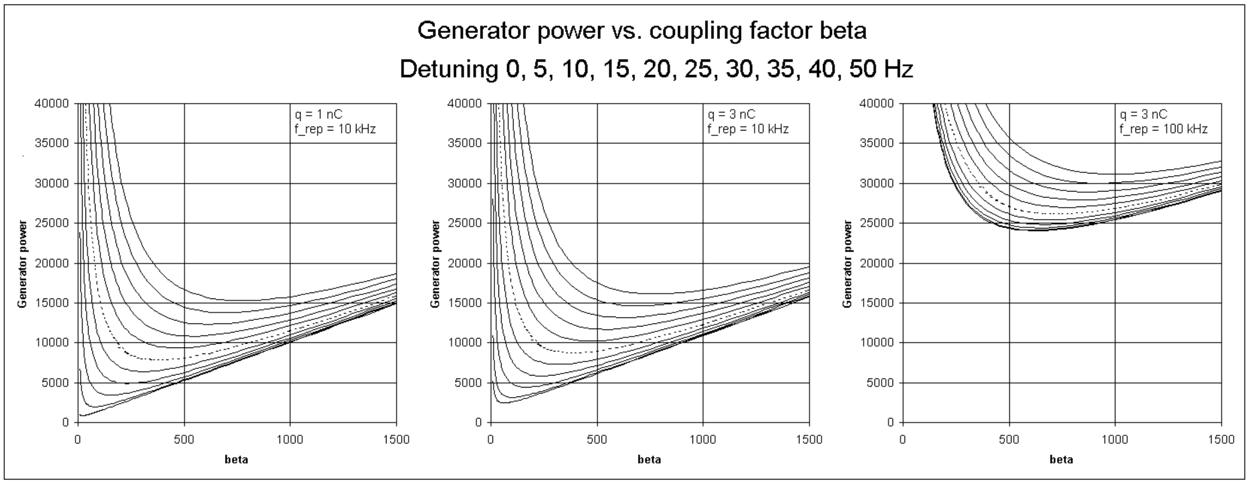

Figure 9-6 Generator power required for 1 nC at 10 kHz, 3 nC at 10 kHz, and 3 nC at 100 kHz, as a function of the coupling factor, and the detuning Δf.

For each detuning there exists an optimum coupling factor that leads to minimum generator power. For a given beam current, the generator power increases for increasing tuning deviation. Figure 9-7 shows the generator power for four beam currents under the assumption that the coupling factor has always been adjusted for the respective highest tuning deviation, i.e. following the minima in Figure 6 above. Not surprisingly, the tuning deviation has a particularly important effect at low beam currents.

The key factors for the nominal detuning of 25 Hz are summarized in Table 9-3 for the three assumed operating scenarios.

Table 9-3 Cavity parameters for nominal detuning 25 Hz

Beam charge	Beam Rep. rate	Beam current	Coupling β_{opt}	Loaded Q Q_l	Loaded BW_L	Generator power
1nC	10 kHz	40 μA	383	$26.0 \cdot 10^6$	50 Hz	7.86 kW
3nC	10kHz	120μA	398	$25.1 \cdot 10^6$	51.9 Hz	8.75 kW
3nC	100kHz	1200μA	750	$13.3 \cdot 10^6$	97.6 Hz	26.15 kW

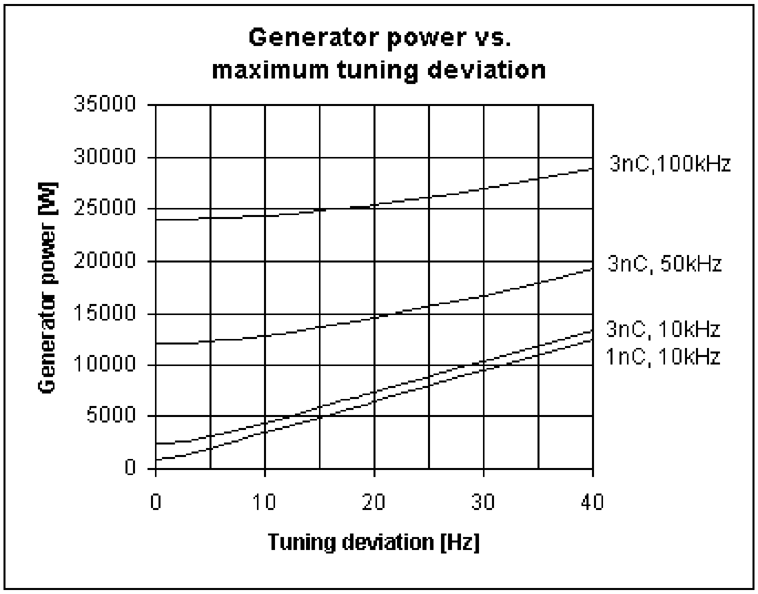

Figure 9-7 Generator power for four beam currents under the assumption that the coupling factor has always been adjusted for the respective highest tuning deviation,

For small beam currents, the optimum loaded bandwidth of the system Q_{Lopt} coincides with 2*□f. In other words the optimum system bandwidth then just holds the two-sided (double single-sided) frequency deviation. With small beam loading and high *Q*, the magnitude of the cavity conductance is almost equal to the reactive component since the resistive part is negligibly small; the matching condition “magnitude of load conductance = generator conductance *1*/*Z*” then leads to this result.

In all three cases the coupling is significantly weaker than in the standard TESLA cavity, where □ = 3332 and $Q_L = 3{\cdot}10^6$. This should be no problem since it means withdrawal or shortening of the capacitive power coupler.

Table 9-4 summarizes the baseline main linac requirements, together with the TESLA pulsed system specifications for comparison.

Table 9-4 Baseline parameters for the recirculating linac, and the TESLA TTF linac specifications

Parameter	Recirculating linac	TESLA
Cavity Length [m]	1.038	1.038
E_{acc} [MV/m]	20	23.4
Frequency [GHz]	1.3	1.3
ZT^2/Q Per Cavity [Ω]	1036	1036
Flat Top [μs]	CW	950
Pulse Length [μs]	CW	1370
Beam Current [mA]	0.04	9.5
Quality Factor Q_0	10^{10}	10^{10}
Beam Repetition Rate [Hz]	10,000	5
Duty Factor	1	0.00685
Beam Power Per Cavity [kW]	0.83	231
Total Beam Power (4 modules) [kW]	26.6	7384
Peak Power Loss Per Cavity [W]	42	57
External Quality Factor Q_{ext}	2.6×10^7	2.5×10^6
Bandwidth [Hz]	50	520
Average RF Power Loss Per Cavity [W]	42	0.39
Average RF Load Per Module [W]	333	3.12
Average Power Loss For 4 Modules [kW]	1.331	0.0125
Peak Input RF Power For 4 modules [kW]	288	7,384

REFERENCES

[1] TESLA Technical Design Report, DESY 2001-011, ECFA 2001-209, TESLAS Report 2001-23, TESLA-FEL 2001-05 (March 2001)

[2] W. Decking, “The TESLA Linear Collider”, 2002 Linear Collider Conference, SLAC, California, USA (Feb. 2002)

[3] The NLC Collaboration edited by N. Phinney, “2001 Report on the Next Linear Collider”, LBNL-PUB-47935, SLAC-R-571 (June 2001)

[4] TESLA Report 98-20, pp. 95-97 and private communication

[5] L.Merminga and J.R.Delayen, CEBAF note TH#96-022